Electricity generation and color removal at sulfate-reducing conditions in microbial fuel cell

Akgul V.[1], Cirik K.[2*], Duyar A.[3], Basak S.[4], Akman D.[1]

[1]Department of Bioengineering and Sciences, Kahramanmaras Sutcu Imam University, Kahramanmaras 46100, Turkey

[2]Department of Environmental Engineering, Kahramanmaras Sutcu Imam University, Kahramanmaras 46100, Turkey

[3]Department of Environmental Engineering, Suleyman Demirel University, Isparta 32260, Turkey

[4]Department of Occupational Health and Safety, Artvin Coruh University, Artvin 08000, Turkey

*to whom all correspondence should be addressed: e-mail: kcirik@ksu.edu.tr

Abstract

The main aim of this study is to investigate the simultaneous azo dye removal and bioelectricity production at sulfate-reducing conditions in a continuously fed dual-chamber microbial fuel cell (MFC). Initially, optimization of sulfate reduction was performed at different sulfate concentrations (100-900 mg/L) and the constant COD of 1000 mg/L, corresponding to COD/sulfate ratio of 1.11-10, and varying HRT of 12-48 h. Optimum COD/sulfate ratio and HRT was found 1.66 and 36 h, respectively, corresponding to 96% COD removal, 44% sulfate removal and yielded about 24 W/m² power density. Further, MFC was fed with azo dye containing (50-1000 mg/L) simulated wastewater to evaluate dye removal performance of sulfate-reducing bacteria. Addition of azo dye slightly enhanced the power production to 26 W/m², the highest value obtained during our study. Sulfate and COD removals were adversely affected at azo dye concentrations over 300 mg/L and 150 mg/L, respectively. Additionally, color removal performance of MFC was excellent however, chemical azo dye reduction out-competed with enzymatic reduction at high azo dye levels (>500 mg/L) leading to a poor sulfate (<15%) and COD (<45%) removal and recovery of azo dye reduction efficiency to 91%.

Keywords: Color, electricity generation, microbial fuel cell, sulfate.

1. Introduction

Microbial fuel cell (MFC) gained considerable interest in recent years for the applications of bioelectricity production along with simultaneous wastewater treatment (Sevda *et al.*, 2013; Majumder *et al.*, 2014). MFC is the device that uses bacteria as the catalysts in the anode to oxidize organic and inorganic matter. In general applications, MFC consists of anode and cathode chambers physically separated by a proton exchange membrane (PEM). Microorganisms attached on the biofilm layer of anode, oxidize organic matter anaerobically and then the electrons flow up from the anode onto the cathode through an external circuit, thus producing electricity (Guerrini *et al.*, 2013). Additionally, the protons enter the cathode chamber where they combine with oxygen (terminal electron acceptor) to form water (Rabaey *et al.*, 2007).

So far, simulated wastewaters containing diverse types of organic substrates and different kinds of wastewaters ranging from domestic wastewater to brewery wastewater (Wen *et al.*, 2009) have been used as an energy source in MFC (Najafpour *et al.*, 2010; Sharma and Li, 2010; Izadi and Rahimnejad, 2013). Additionally; previous MFC studies showed that the MFC can be also used for the treatment of biorefractory wastewater along with other degradable co-substrates (Su *et al.*, 2013; Yong *et al.*, 2014). One of most studied biorefractory compounds is azo dye characterized by -N=N- which represents the largest class of dyes used in textile-processing. Biodegradation of azo dyes is difficult due to their complex structure and synthetic nature, and hence these compounds are one of the most problematic contaminants in textile industry (Li *et al.*, 2016). However, previous studies showed that the azo bonds can be broken biologically by some anaerobes. The reduction of azo dyes under anaerobic condition is based on oxidation–reduction reactions in which the dye acts as the final electron acceptor while organic matter acts as the electron donor (Xu *et al.*, 2016; Yang *et al.*, 2016).

In this study, the azo dye and sulfate were selected as main contaminants. Sulfate largely presents in textile coloring wastewaters through its use in dye baths for ionic strength adjustment or as a leaving group from vinyl-sulphone reactive dye fixation onto cotton fibers (Albuquerque *et al.*, 2005). Additionally, the use of H_2SO_4 in pH control provides an important contribution to sulfate availability. Several earlier studies investigated the possibility of MFCs for removal of azo dyes in simulated wastewater (Kong *et al.*, 2013; Yong *et al.*, 2014), however; there is a lack of information about the role of sulfate-reducing conditions on the azo dye reduction and

electricity production in MFC. The biological sulfate reduction process is mediated by a group of microorganisms known as sulfate reducing bacteria (SRB) that use sulfate as electron acceptor. As anaerobic color removal occurs by the way of reduction of the azo dye which acts as a final electron acceptor in the microbial electron transport chain, color removal may be either stimulated or competitively suppressed in the presence of sulfate. Therefore, MFC was tested in the availability of sulfate and azo dye under different operating conditions to reveal the bioelectricity production of MFC by sulfate-reducing bacteria.

2. Materials and methods

2.1. Simulated wastewater and inoculum source

The MFC anode was inoculated with anaerobic sludge from a full-scale anaerobic digester located at Gaziantep, Turkey. The anode chamber was fed continuously with synthetic wastewater containing (per liter) 4 g $NaHCO_3$, 0.6 g NH_4Cl, 9.3 g $NaH_2PO_4 \cdot H_2O$, 3.2 g Na_2HPO_4, 0.125 g K_2HPO_4, 0.11 g $CaCl_2 \cdot 2H_2O$, 0.5 g cyctein HCl, minor amounts of metal ions (Fe, Zn, Co, Cu, Mn and Ni) and vitamins. Acetate, contributed to 1000 mgCOD/L, was used to provide a readily biodegradable carbon source for MFC. Both magnesium sulfate and sodium sulfate were used as sulfate source. The studied azo dye was the monoazo reactive dye Remazol Brilliant Violet 5R (C.I Reactive Violet 5), (Sigma–Aldrich, Germany). The synthetic wastewater was prepared daily.

2.2. Microbial fuel cell design and operation

Schematic views and photograph of the dual-chamber MFC used in the experiments are shown in shown in Figure 1A and 1B, respectively.

The technical characteristic and operation procedures of the MFC are the same as previously used MFC (Cirik, 2014). The electrode was Pt (effective surface area for biofilm growth was 32 cm^2), which has been widely used in MFC technology. In order to minimize the internal resistance involved with ohmic loses, both electrodes were placed in direct contact with the proton exchange membrane. The electrodes were connected with copper wire through a resistance of 10 Ω during the experiment.

The synthetic wastewater was continuously pumped into the anode chamber using a peristaltic pump (Masterflex L/S, Cole-Parmer 7524-45, USA). The anode chamber was sparged with nitrogen to remove oxygen to ensure anaerobic condition during the MFC operation. All experiments were carried out at uncontrolled pH and the constant temperature of 30±2°C. The cathode chamber was aerated continuously using air pumps to provide oxygen as the terminal electron acceptor.

The performance of the MFC was evaluated for around 570 days in three different parts (Table 1). Optimization of sulfate-reducing conditions in the MFC system was performed in the first two parts, while the last part mainly

related to the azo dye reduction studies under sulfate-reducing conditions. The operational conditions were changed after observing steady state measurements in COD, sulfate and azo dye concentrations.
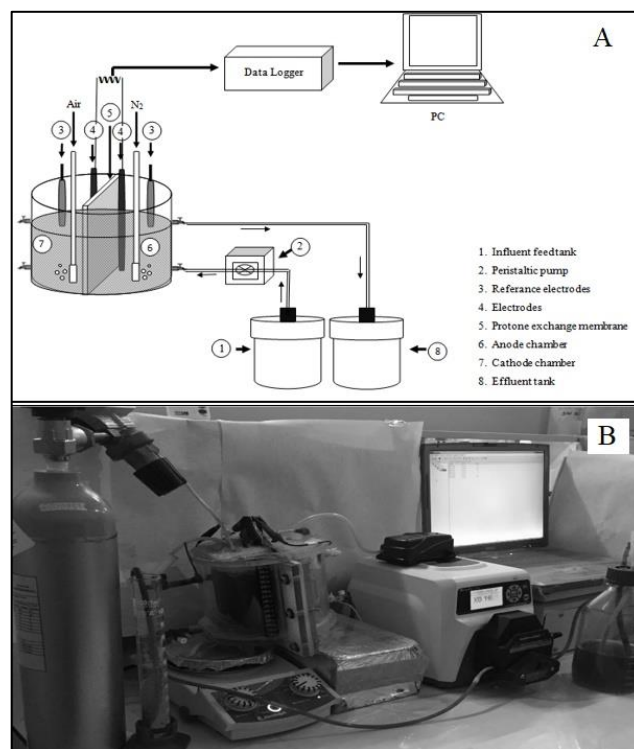

Figure 1. Schematic view of dual-chamber MFC (A), Photograph of the dual-chamber MFC used in the experiments (anode chamber on the left; cathode chamber on right) (B)

The details of each partare shown in Table 1. In the first part (days 0-133), the effect of varying COD/sulfate ratio(10-1.11) was evaluated at constant HRT of 24 hours. During part II (days 158-267), HRT was increased stepwise from 12 h to 48 h at optimum COD/sulfate ratio of 1.66. In the last part of the study, Remazol Brilliant Violet 5R (C.I Reactive Violet 5) (Sigma–Aldrich, Germany) was included to the feed solution to provide influent azo dye concentrations of 50-1000 mg/L. The reactor was sampled 3 times a week for performance evaluation. All assays were run in triplicate and mean values were presented.

2.3. Analyses

Samples were firstly filtered through a pre-washed filter paper through 0.45 μm pore-sized syringe filter (Sartorius AG, Gottingen, Germany) to remove biomass and other particles. Azo dye concentrations were measured spectrophotometrically with a Shimadzu UV-1601 Spectrophotometer at 560 nm using the experimentally derived calibration curve ($ABS_{560nm}=0.0138 \cdot Conc._{azodye} + 0.005$; $R^2=0.9999$). Intermediates of RBV-5R were analyzed using an HPLC system equipped with SPD-M20A diode array detector (DAD) (Shimadzu Co. Kyoto, Japan) and Inertsil ODS-3V (250 mm × 4.6 mm ID 5 μm) column.

Table 1. Operational conditions of MFC

Parts	Periods	Days	COD (mg/L)	Sulfate (mg/L)	COD/sulfate ratio	HRT (hour)	Azo dye (mg/L)
Part 1. Effect of COD/Sulfate ratio	I	(0-133)	1000	100	10	24	-
	II			300	3.33		
	III			600	1.66		
	IV			900	1.11		
Part 2. Effect of HRT	I	(158-267)	1000	600	1.66	12	-
	II					24	-
	III					36	-
	IV					48	-
Part 3. Effect of azo dye concentration	I	(317-569)	1000	600	1.66	36	50
	II						100
	III						150
	IV						200
	V						300
	VI						500
	VII						750
	VIII						1000

Aromatic amine standards were generated with the use of sodium dithionite ($Na_2S_2O_4$) for the cleavage of the –N=N– linkage followed by HPLC analysis of the reduction products of RBV-5R. Chemical reduction was performed for 5 min at 70°C with a dithionite/color (w:w) ratio of 10. Dissolved sulfide concentration was determined with the use of a Shimadzu UV-1601 Spectrophotometer. COD and alkalinity were determined according to APHA standard methods (APHA, 1999). Samples were acidified with concentrated H_2SO_4 to below pH 2 and purged with N_2 gas for approximately 5 min to remove H_2S prior to COD determination. An ion chromatography (Dionex ICS-3000, Sunnyvale, CA, USA) equipped with Ion Pac AG19 guard and AS19 analytical columns were used to measure the sulfate concentrations. The pH of each chamber was measured using multimeter (WTW340I Weilheim, Germany). The ORP level between anode and cathode compartments was measured by Ag/AgCl reference electrode (BASI, MF-2052).The voltage (V) across an external resistance (10 Ω) in the MFC circuit was on-line monitored at 60-min intervals using an online data acquisition system.

2.4. Calculations

Voltage data acquisition from MFC was conducted using a Fatek programmable controller data logging system. The current (I) flowing through the external circuit was calculated using the Ohm's law, where V is the measured voltage, and R (ohm) is the external resistance (Eq. 1).

$$I(A) = \frac{V}{R} \qquad (1)$$

Measured electrical voltage across the load and the current converted to power, P (watt), according to (Eq. 2).

$$P(watt) = V.I = I^2.R \qquad (2)$$

Power density, P_{An} (W/m^2), was normalized by the cross-sectional area of the studied electrode in the anode chamber.

Coulombic efficiency reflects the ratio of the number of electrons passing through the external load, which generates electricity, to the number of electrons removed from the substrate during bio conversion. The coulombic efficiency (ηCE) of continuous flow MFC was calculated as follows (Eq. 3) (Liu and Logan, 2004):
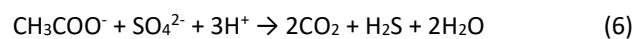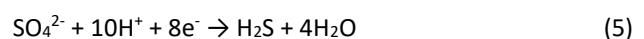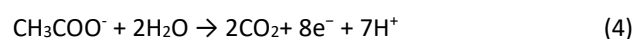
$$\eta CE = \frac{I}{F \cdot \left(\frac{4}{32} \right) \cdot \Delta COD \cdot Q_{in}} \qquad (3)$$

where I is the current (A), F is the Faraday constant (96.485 C/mol.e$^-$), 4 is the electron number gained by the reduction reaction of 1 M O_2, 32 is the molar mass of O_2, Q_{in} is volumetric influent flow rate of MFC (L/s), ΔCOD is the difference of chemical oxygen demand (COD) between influent and effluent.

3. Results and discussion

3.1. Effect of COD/sulfate ratio on MFC performance

This part of the study was composed of four periods in which MFC was fed with azo dye free wastewater to enrich acetate-oxidizing sulfate-reducing bacteria (SRB) at varying COD/sulfate ratios. Normally, sulfate is biologically reduced under anaerobic conditions and eight electrons are used to produce sulfide while acetate is oxidized to carbon dioxide as shown in the following reactions (Eqs. 4-6):

$$CH_3COO^- + 2H_2O \rightarrow 2CO_2 + 8e^- + 7H^+ \qquad (4)$$

$$SO_4^{2-} + 10H^+ + 8e^- \rightarrow H_2S + 4H_2O \qquad (5)$$

$$CH_3COO^- + SO_4^{2-} + 3H^+ \rightarrow 2CO_2 + H_2S + 2H_2O \qquad (6)$$

According to the above reactions, stoichiometric value for sulfate reduction is equal to COD/sulfate ratio of 0.67 which is lower than COD/sulfate ratios used in this study. It should be noted that there was no apparent carbon limitation for sulfate reduction in MFC reactor.

The value of 0.67 is recommended as adequate for SRB, while a higher ratio than 2.7 is favorable to methane-producing bacteria (Chen and Cheng, 2008).

To evaluate the effect of COD/sulfate ratio on reactor performance the influent COD was kept constant at 1000 mg/L and sulfate concentration in the feed was increased stepwise from 100 mg/L to 900 mg/L, corresponding to COD/sulfate ratio of 10-1.1 (Table 1). The COD removal, bioelectricity production and sulfate removal performances of MFC system are shown in Figure 2A, B and C, respectively. In the first period, MFC was operated at COD/sulfate ratio of 10, corresponding to 1000 mg/L and 100 mg/L influent COD and sulfate concentrations, respectively. Sulfate and COD removal efficiencies were about 48% and 74%, and bioelectricity production was 25 W/m^2 during the first period (Figure 2). Dissolved sulfide was observed about 10 mg/L in the effluent. Increase in influent sulfate concentration to 300 mg/L (Period II) and 600 mg/L (Period III), corresponding to COD/sulfate ratio to 3.3 and 1.66, respectively; had a positive effect on COD removal efficiency which was approached to 90% and 98%, respectively. However, further decrease in COD/sulfate ratio to 1.1 in the last period (Period IV) did not change COD removal efficiency, which was about 98% (Figure 2A). Although COD in the feed was always higher than the stoichiometric requirement (COD/sulfate=0.67), sulfate removal efficiency decreased to 40%, 35%, and 24% in periods II, III and IV when sulfate concentration in the feed was increased to 300 mg/L, 600 mg/L, and 900 mg/L, respectively. In this study, COD/sulfate ratio of 1.66 was found optimum in terms of high COD removals (98%) and bioelectricity production. In a study performed by Ghangrekar *et al.* (2010) obtained lower COD removal compared to our study which was about 79% at the COD/sulfate ratio of 0.8.

The COD removal in subsequent period (period IV) was similar however, energy production was lower. Sulfide production in the first period was low being 10 mg/L but then gradually increased parallel to decreased COD/sulfate ratio and reached to 18 mg/L, 25 mg/L, 30 mg/L, in periods II, III and IV, respectively, supporting sulfate removal data (Figure 2C). The predominant sulfur compound was HS at the pH levels in the anode compartment (8.0-8.5). However, there was a discrepancy in the balance of sulfur compounds between the amount of sulfate removed and sulfide generated. Possibility of sulfide diffusion toward the cathode compartment was eliminated by proton exchange membrane since sulfide was not detected in cathode effluent. Previous studies demonstrated that produced sulfide could be oxidized at the anode to elemental sulfur, thiosulfate or sulfate (Sun *et al.*, 2010; Lee *et al.*, 2012). Elemental sulfur (S^0) formation observed during MFC operation confirmed the sulfide oxidation and part of sulfide loss can be explained by such a mechanism.

The bioelectricity production went up with the rise of influent sulfate concentration from 100 mg/L (Period I) to 300 mg/L (Period II), which was increased from 25 W/m^2 to 27 W/m^2, respectively (Figure 2B). However, further increase in influent sulfate concentration adversely affected the bioelectricity generation, which dropped to 23 W/m^2 and 22 W/m^2 in periods III and IV, respectively. The power density obtained in our study was relatively higher compared to previous studies (Zhao *et al.*, 2009; Ghangrekar *et al.*, 2010).

Anode alkalinity is produced as a result of sulfate reduction coupled with organic carbon oxidation (Eqs. 4-6) (Ozdemir *et al.*, 2013). The alkalinity production in the anode was about 877 mgCaCO$_3$/L at period I. In subsequent periods, alkalinity production slightly decreased to 780, 770, and 765 mgCaCO$_3$/L in periods II, III, and IV, respectively. This was due to the increased carbon dioxide production since COD removals were higher in these periods. Conversely, cathode influent pH of 6.85 decreased slightly to 6.68 during MFC operation. This was due to the movement of H$^+$ ions from the anode to cathode, which is typically observed in an MFC. Coulombic efficiency (ЄC) was the fraction of electrons (charge) that contribute to electricity generation and affected from the anode feed exists in the MFC system.
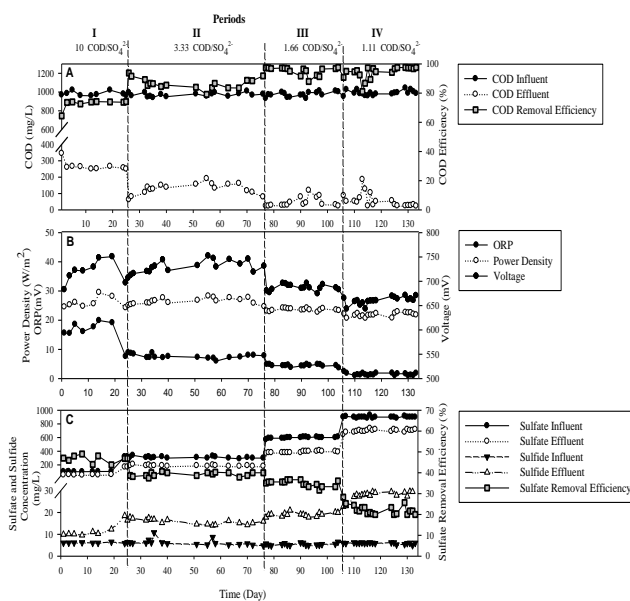

Figure 2. COD removal (A), voltage-power generation (B), and sulfate-sulfide profiles (C) observed in dual-chamber MFC

Generally, the observed ЄC values in MFCs inoculated with mixed cultures and operated with real wastewater were relatively lower compared to simulated wastewaters (Lefebvre and Al-Mamun, 2008). In our study, coulombic efficiency was 18% in the first period and decreased to 15.3; 12.8; and 12.5% when feed sulfate concentration increased from 100 to 300, 600, and 900 mg/L (10 Ω), in periods II, III, and IV; respectively. Similarly, in a study

performed by Zhao *et al.* (2018), obtained EC values was between 10.0 -12.5%.

3.2. Effect of HRT on MFC performance

HRT was increased stepwise from 12 h to 48 h at optimum COD/sulfate ratio of 1.66 obtained from the first part of the study. Additionally, COD and sulfate concentrations were kept constant at 1000 mg/L and 600 mg/L during this study part, respectively.

In the first period, continuously-fed MFC was operated with HRT of 12 h and COD removal efficiency was reached to 79% (Figure 3A). Produced sulfide concentration as a result of biological sulfate reduction was around 18.8 mg/L and the maximum sulfate removal observed in this period was about 26%, which indicated that the HRT remained inadequate for sulfate reduction activity, corresponding to 445 mg/L effluent sulfate concentration (Figure 3C). Additionally, the maximum power density of 21 W/m^2 was obtained in this study period, corresponding to a cell voltage of 640 mV (Figure 3B). In the subsequent two periods (period II and III), HRT was increased stepwise to 24 h and 36 h, respectively. In these periods, COD removal efficiency prominently increased and reached around 96%, corresponding to effluent COD concentration of around 30 mg/L (Ge *et al.*, 2013). The increasing HRT from 12 h to 24 h and 36 h slightly increased cell voltage which approached to 675 mV and 690 mV, respectively. The maximum power density of 24 W/m^2 was obtained in the period III at HRT of 36 h. The results indicated that high HRT was in favour of increasing power generation in dual-chamber MFC and the HRT of 36 h was found optimum for high MFC performance.
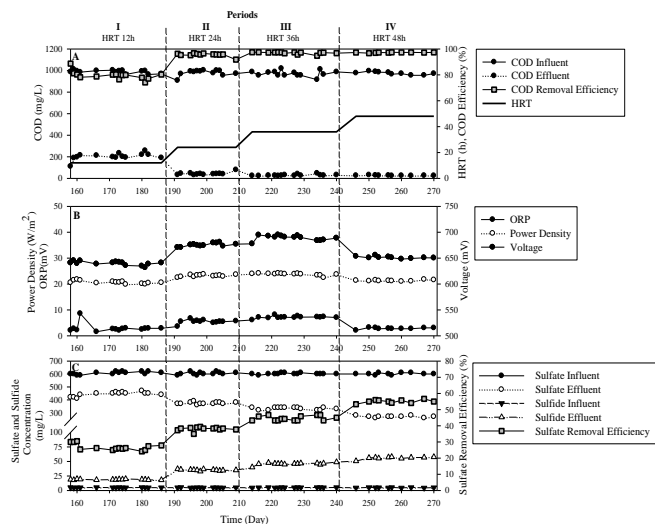

Figure 3. COD removal (A), voltage-power generation (B), and sulfate-sulfide profiles (C) observed in dual-chamber MFC

Additionally, the increase in the bioelectricity production was due to the sufficient contact time between electron donor and bacteria related to high HRT (Figure 3A and 3B). When HRT was increased to 24 h and 36 h, sulfate removal increased and reached to 38% and 44% in the periods II-III, respectively. Dissolved sulfide concentration

incrementally reached to 35.2 mg/L and 46.9 mg/L, respectively. In the last period, MFC was operated at HRT of 48 h. Significant variation in the effluent COD concentration was not observed compared to period III, corresponding to 27 mg/L and 97.2% removal efficiencies respectively. Increasing HRT resulted in improvement of sulfate removal efficiency which was 55% in period IV (Figure 3C). The increase sulfate profile can be explained that microorganisms responsible for anaerobic sulfate reduction has a relatively low growth rate, and thus long HRT level was increased microbial activity of SRB (Cirik *et al.*, 2013). Sulfate removal and sulfide generation had a similar profile and compatible with each other. Sulfide production in the anode chamber of MFC reached to 60 mg/L, supporting sulfate removal data in the last period (Figure 3C). Very high HRT levels (≥48 h) adversely affected MFC performance in terms of bioelectricity generation and power density, which was decreased from 24 W/m^2 to 21 W/m^2 (Figure 3B). Coulombic efficiency observed in our study was 7.4% in the first period and increased to 13, and 17.3% when HRT increased from 12 h to 24 h, and 36 h, in periods II, and III, respectively. The maximum coulombic efficiency of 24% was obtained in the last period at HRT of 48 h.

Acetate oxidation, sulfate reduction, and proton exchange membrane properties are the main factors responsible for variance in pH and alkalinity. pH increment was observed as a result of sulfate reduction coupled with organic carbon oxidation. Additionally, the formation of organic acids and releasing of hydrogen ions during the anodic reaction (organic matter fermentation) decreased pH value in the anode chamber (Akman *et al.*, 2013; Akman *et al.*, 2014). Anode influent pH value was kept constant at 5.1 throughout the MFC operation. pH tended to increase at the first two periods and this increment was probably resulted from increasing sulfate removal efficiency at high HRT levels (Figure 3C). However, the significant increase in pH value was never observed in the periods III and IV, although sulfate removal efficiency was higher than other periods (period I and II) as a result of high performance of the proton exchange membrane (high proton diffusion rate through the membrane). Anode alkalinity values gradually increased from 624 mgCaCO$_3$/L to 757 mgCaCO$_3$/L during all periods (periods I-IV) as a result of sulfate reduction and simultaneous organic carbon oxidation in the anode chamber. Influent cathode pH value was about 6.85. Effluent pH and alkalinity values of the cathode chamber were not affected from varying HRT due to the daily change with distilled water of the cathode content, corresponding to 6.5 pH and 10.5 mgCaCO$_3$/L alkalinity.

3.3. Effect of azo dye concentration on MFC performance

In this part of the study, MFC was operated under sulfate-reducing conditions at different initial dye concentrations (50-1000 mg/L). COD/sulfate ratio was 1.66 (Table 1). Additionally, HRT was kept constant at 36 h during study periods. The profiles of COD, sulfate, azo dye removal and bioelectricity production were shown in Figure 4.
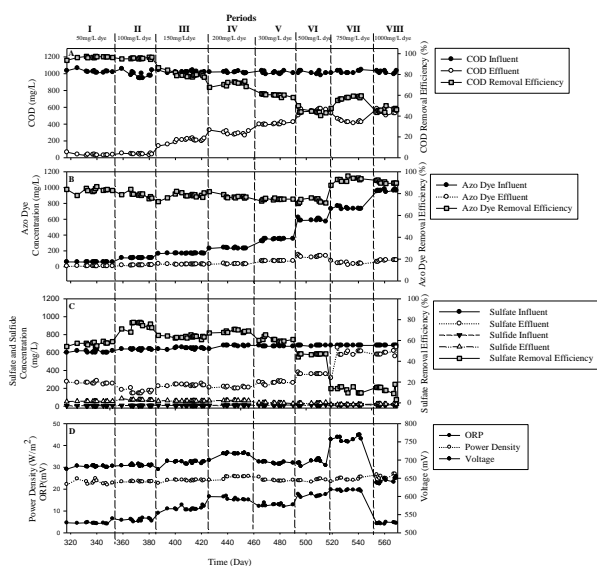
Figure 4. COD removal (A), azo dye concentration (B), sulfate-sulfide profiles (C) and voltage-power generation (D) observed in dual-chamber MFC

Since anaerobic azo dye reduction is an oxidation–reduction reaction, a liable electron donor is essential to achieve high color removal rates. Acetate in the synthetic wastewater acted electron donor source for both sulfate and azo dye reductions, corresponding to 1000 mg/L influent COD. COD removal was 96% in the first period and decreased when influent azo dye concentration was increased. The observed COD removals in periods II-VIII were 95, 80, 71, 60, 44, 56, and 45%, respectively (Figure 4A).

As azo bond cleavage –N=N– involves a transfer of four-electrons (reducing equivalents), one-mole azo dye equals to 32 gCOD, corresponding to 0.043 gCOD/g azo dye (RBV-5R). Hence, the COD requirement for azo dye reduction even at the highest azo dye concentration (1000 mg/L) was calculated as 43 mgCOD/L. Some proportion of the substrates could be consumed for azo dye reduction, however, for a real perspective application, the COD demand of azo dye reduction to be negligible, and therefore there may be different factors responsible for decreasing COD removal efficiencies. One could be due to the toxic effects of azo dye and its breakdown products on the microorganism, another could be due to the aromatic amines that form due to cleavage of the –N=N– bond of RBV-5R contributed the residual COD, resulting in low COD removals.

The variations of azo dye concentrations in the sulfate-reducing MFC are presented in Figure 4B. In the first period dye removal efficiency was 83% and decreased linearly proportional to increased influent dye concentration during periods II, III, IV, V, and VI corresponding to 78.8; 78.2; 76; 74.8; and 73.5% dye removal efficiencies; respectively. However, further increase in dye concentrations to 1000 mg/L; an unexpected improvement on dye removal was observed, corresponding to 92 and 91% azo dye removal efficiency which was similar to previously published studies (Marin *et al.*, 2018; Sun *et al.*, 2009). The high azo dye

reduction by SRB may occur enzymatically or chemically with the sulfide produced during dissimilatory sulfate reduction. There may be two processes in this study responsible for azo dye removal: (i) chemical reduction by biologically produced sulfide and (ii) enzymatic reduction. In enzymatic azo dye reduction both influent COD (organic matter) and azo dye are expected to be reduced simultaneously, therefore chemical reduction seems dominant mechanism responsible for azo dye reduction as COD removal was relatively dropped.
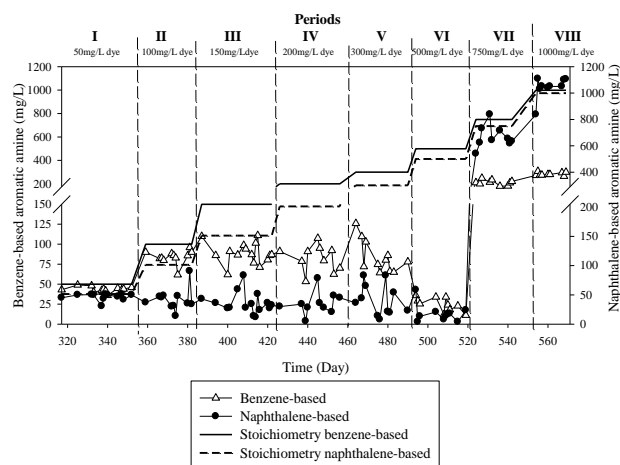

Figure 5. Benzene and naphthalene-based aromatic amine profiles observed in dual-chamber MFC

Sulfate removal was initially increased from 56 to 74% by increasing influent azo dye to 100 mg/L (period II) however it decreased stepwise and dropped to 12% when influent azo dye concentration was 1000 mg/L which was the maximum azo dye concentration tested during this study (period VIII). Considering that the required amount of organic matter for azo dye reduction was quite lower than that for sulfate reduction, which was discussed above, the decrease of sulfate reduction should be due to toxic effects of azo dyes and breakdown products on the microorganism. Sulfide productions were parallel to sulfate removals supporting sulfate removal data (Figure 4C), however discrepancy in the balance of dissolved sulfide and reduced sulfate were again observed. The observed elemental sulfur was the main reason as discussed above. Similarly, Zhang *et al.* (2008), proposed the possibility to utilize the sulfate-reducing bacteria to convert sulfate to sulfide, then the MFC to convert the formed sulfide to elementary sulfur. Electricity production was slightly accelerated however it was relatively stable about 24-26 W/m^2 compared to other operational parameters. Coulombic efficiency (10 Ω), was 17.2% in the first period and increased to 17.6; 21; 24.9; 28; 38; 33; 34% when feed azo dye concentration increased from 50 to 100, 150, 200, 300, 500, 750 and 1000 mg/L in periods II-VIII; respectively. As a result, increasing dye concentration increased the recovery of electrons. However, after dye concentration was increased to 1000 mg/L, the voltage generation was decreased from 700-780 mV to 650 mV. Similar results were reported by Marin *et al.* (2018). The chemically

reduced Remazol Brilliant Violet 5R products were used as aromatic amine standard due to the unavailability of true standards. There were two main peaks in HPLC measurements corresponding to the benzene-based and naphthalene based aromatic amines. An examination of the HPLC analyses results in Figure 5 reveals that the formation of aromatic amines indicates azo dye reduction. This suggests that bacterial cultures can reduce azo dyes and produce aromatic amines at sulfate reducing conditions. Stoichiometric values of formed products for each azo dye concentration applied were also added. Actually, accumulation of aromatic amines was expected since they are generally persisted to anaerobic conditions and tend to accumulate to toxic levels (Yasar *et al.*, 2012). However, aromatic amine concentrations were always below stoichiometric values reflecting the removal of aromatic amines by attached anaerobes on sulfate reducing anodic electrode. It seems that this attached growth provides the biological removal of aromatic amines by facilitating the growth of specific microorganisms in high sludge ages which is in favor of low growing rate microorganism. There are few reports in literature related to aromatic amine degradation under sulfate reducing conditions. Increase in azo dye concentration resulted in increased aromatic amine removal. Benzene based aromatic amine removal was 13% in the period I and reached to 95% in periods VI. Similarly, naphthalene based aromatic amine removal was 97% in period VI. However, between days 520 and 569 (period VII-VIII), increased aromatic amine formation was observed rather than removal especially for naphthalene-based amine (Figure 5). This was probably due to the toxic effect of azo dye on microorganism since in these periods (VII and VIII) all biological parameters were fallen down. Alkalinity production was lower compared to previous parts and tended to decrease as dye loading was increased. Alkalinity production in period I was 637 mgCaCO$_3$/L at 50 mg/L dye concentration then dropped to 478 mgCaCO$_3$/L in period VIII. The effluent pH of the anode (periods I-VI) was close to 8.0-8.6 throughout the reactor operation although the feed pH was relatively low as 5.1. However, lower pH values observed in periods VII and VIII were probably due to the adverse effect of dye on microorganism activity.

4. Conclusion

In this study, the sulfate reducing MFC system has been successfully operated for simultaneous sulfate and dye removal. Under dye free conditions optimum COD/sulfate ratio and HRT were 1.66 and 36 h, respectively; corresponding to 96% COD, 44% sulfate removal and yielded about 24 W/m^2 power density. MFC was successful for simultaneous reduction of sulfate and azo dye. Surprisingly 97% removal of break down products was achieved by sulfate reducing anaerobes. High azo dye concentrations (>500 mg/L) adversely affected biological parameters (COD, sulfate and aromatic amine), while dye removal and power density reached to highest values of 92% and 26 W/m^2, respectively.

References

Akman D., Cirik K., Ozdemir S., Ozkaya B., Cinar O. (2013), Bioelectricity generation in continuously-fed microbial fuel cell: Effects of anode electrode material and hydraulic retention time, *Bioresource Technology*, **149**, 459–464.

Akman D., Ozdemir S., Cirik K., Ozkaya B., Cinar O. (2014), Effect of some operational parameters in fed-batch microbial fuel cells for electricity generation. *Research Journal of Chemistry and Environment,* **18(3)**, 87–93.

Albuquerque M.G.E., Lopes A.T., Serralheiro M.L. (2005), Biological sulphate reduction and redox mediatör effects on azo dye decolourisation in anaerobic–aerobic sequencing batch reactors. *Enzyme and Microbial Technology,* **36**, 790–799.

APHA (1999), Standard Methods for the Examination of Water and Wastewater, 20th ed., American Public Health Association/American Water Works Association/Water Environment Federation, Washington, DC, USA.

Chen Y., Cheng J.J., Creamer K.S. (2008), Inhibition of anaerobic process: a review. *Bioresource Technology* **99**, 4044–4046.

Cirik K., Dursun N., Sahinkaya E., Cinar O. (2013), Effect of electron donor source on the treatment of Cr(VI)-containing textile wastewater using sulfate-reducing fluidized bed reactors (FBRs). *Bioresource Technology* **133**, 414–420.

Cirik K. (2014), Optimization of bioelectricity generation in fed-batch microbial fuel cell: effect of electrode material, initial substrate concentration, and cycle time. *Applied Biochemistry and Biotechnology*, **173(1)**, 205–214.

Ge Z., Ping Q., Xiao L., He Z. (2013), Reducing effluent discharge and recovering bioenergy in an osmotic microbial fuel cell treating domestic wastewater. *Desalination* **312**, 52–59.

Ghangrekar M.M., Murthy S.S.R., Behera M., Duteanu N. (2010), Effect of sulfate concentration in the wastewater on microbial fuel cell performance. *Environmental Engineering and Management Journal*, **9**, 1227–1234.

Guerrini E., Cristiani P., Trasatti S.P.M. (2013), Relation of anodic and cathodic performance to pH variations in membraneless microbial fuel cells. *International Journal of Hydrogen Energy*, **38(1)**, 345–353.

Izadi P., Rahimnejad M. (2013), Simultaneous electricity generation and sulfide removal via a dual chamber microbial fuel cell. *Biofuel Research Journal* **1**, 34–38.

Kong F.Y., Wang A.J., Liang B., Liu W.Z., Cheng H.Y. (2013), Improved azo dye decolorization in a modified sleeve-type bioelectrochemical system. *Bioresource Technology* **143**, 669–673.

Lefebvre O., Al-Mamun A., Ng H.Y. (2008), A microbial fuel cell equipped with a biocathode for organic removal and denitrification. *Water Science & Technology* **58**, 881–885.

Li Y., Yang H., Shen J., Mu Y., Yu H. (2016), Enhancement of azo dye decolourizationina MFC-MEC coupled system. *Bioresource Technology*, 202, 93–100.

Majumder D., Maity J.P., Tseng M.J., Chen H.R., Chen C.C., Chang Y.F., Yangand T.C., Chenet C.Y. (2014), Electricity generation and wastewater treatment of oil refinery in microbial fuel cells using Pseudomonasputida. *International Journal of Molecular Sciences*, **15**, 16772–16786.

Marin W., Jang J., Nawaz M., Shahzad A., Lee D.S. (2018), Sulfate-reducing mixed communities with the ability to generate bioelectricity and degrade textile diazo dye in

microbial fuel cells. *Journal of Hazardous Materials*, **352**, 70–79.

Najafpour G., Rahimnejad M., Mokhtarian M., Ramli W.D., Ghoreyshi A. (2010), Bioconversion of whey to electrical energy in a biofuel cell using Saccharomyces cerevisiae. *World Applied Sciences Journal*, **8**, 1–5.

Ozdemir S., Cirik K., Akman D., Sahinkaya E., Cinar O. (2013), Treatment of azo dye-containing synthetic textile dye effluent using sulfidogenic anaerobic baffled reactor. *Bioresource Technology*, **146**, 135–143.

Rabaey K., Rodriguez J., Blackall L., Keller J., Gross P., Batstone D., Verstraete W., Nealson K.H. (2007), Microbial ecology meets electrochemistry: electricity-driven and driving communities. *The ISME Journal*, **1**, 9–18.

Sevda S., Dominguez-Benetton X., Vanbroekhoven K., De Wever H.,Sreekrishnan T.R., Pant D. (2013), High strength wastewater treatment accompanied by power generation using air cathode microbial fuel cell. *Applied Energy*, **105**, 194–206

Sharma Y., Li B. (2010), The variation of power generation with organic substrates in single-chamber microbial fuel cells (SCMFCs). *Bioresource Technology*, **101**, 1844–1850.

Su X.Y., Tian Y., Sun Z.C., Lu Y.B., Li Z.P. (2013), Performance of a combined system of microbial fuel cell and membrane bioreactor: Wastewater treatment, sludge reduction, energy recovery and membrane fouling, *Biosensors and Bioelectronics*, **49**, 92–98.

Sun J., Hu Y., Bi Y.Z., Cao Y.Q. (2009), Simultaneous decolorization of azo dye and bioelectricity generation using a microfiltration membrane air-cathode single-chamber microbial fuel cell. *Bioresource Technology*, **100,** 3185–3192.

Wen Q., Wu Y., Cao D.X., Zhao L.X., Sun Q. (2009), Electricity Generation and modeling of microbial fuel cell from continuous beer brewery wastewater. *Bioresource Technology*, **100(18)**, 4171–4175.

Xu F., Mou Z., Geng J., Zhang X., Li C.Z. (2016), Azo dye decolorization by a halotolerant exoelectrogenic decolorizer isolated from marine sediment. *Chemosphere*, **158**, 30–36.

Yang L., Yang H.Y., Shen J.Y., Yang M., Yu H.Q. (2016), Enhancement of azo dye decolourization in a MFC–MEC coupled system. *Bioresource Technology*, **202**, 93–100.

Yasar S., Cirik K., Cinar O. (2012), The effect of cyclic anaerobic–aerobic conditions on biodegradation of azo dyes. *Bioprocess and Biosystems Engineering*, **35**, 449–457.

Yong XY., Feng J., Chen YL., Shi DY., Xu YS., Zhou J., Shu YW., Xu L., Yong C.Y., Sun Y.M., Shi C.L. (2014), Enhancement of bioelectricity generation by cofactor manipulation in microbial fuel cell. *Biosensors and Bioelectronics* **56**, 19–25.

Zhang L., De Schryver P., De Gusseme B., De Myynck W., Boon N., Verstraete W. (2008), Chemical and biological technologies for hydrogen sulfide emission control in sewer systems: a review. *Water Res.* **42**, 1–12.

Zhao F., Rahunen N., Varcoe JR., Roberts AJ., Avignone-Rossa C., Thumser AE., Slade RCT. (2009), Actor affecting the performance of microbial fuel cells for sulfur pollutants removal. *Biosensors and Bioelectronics* **24**, 1931–1936.

Zhao N., Jiang Y., Alvarado-Morales M., Treu L., Angelidaki I., & Zhang Y. (2018), Electricity generation and microbial communities in microbial fuel cell powered by macroalgal biomass. *Bioelectrochemistry*, **123**, 145–149.